International Journal of Multidisciplinary Research and Development Adsorption of rhodamine b from aqueous solution using mangroves (Rhizophora mucronata) carbon nanotubes nanocomp…

Article · April 2021

CITATION
1

READS
147

4 authors, including:

Eric Njagi
Chuka University College
23 PUBLICATIONS **1,424** CITATIONS

SEE PROFILE

Ochieng Ombaka
Chuka University College
29 PUBLICATIONS **129** CITATIONS

SEE PROFILE

International Journal of Multidisciplinary Research and Development
Online ISSN: 2349-4182, Print ISSN: 2349-5979; Impact Factor: RJIF 5.72
Received: 14-01-2021; Accepted: 06-02-2021; Published: 04-03-2021
www.allsubjectjournal.com
Volume 8; Issue 3; 2021; Page No. 05-10

Adsorption of rhodamine b from aqueous solution using mangroves (*Rhizophora mucronata*) carbon nanotubes nanocomposites

Fidelis Ngugi[1], Joel Mwangi[2], Eric Njagi[2], Ochieng Ombaka[2]
[1] Department of Physical Sciences, Tharaka University College, Marimanti, Kenya
[2] Department of Physical Sciences, Chuka University, Chuka, Kenya

Abstract
The use of dyes has increased dramatically and uncontrollably in last few decades. Different types of dyes are frequently employed in plastics, paper, cosmetics, leather, and textile industries for coloring purposes. These dyes are released in water as effluents, which are of low Biological Oxygen Demand (BOD) and high Chemical Oxygen Demand (COD). Some of these dyes also are toxic and carcinogenic in nature. This study report on the synthesis of Mangroves Roots-Carbon Nanotubes (MRC-CNT) nanocomposite as an adsorbent for efficient removal of Rhodamine B (Rh. B) dye from aqueous solution. Effect of contact time, initial concentration of dye, pH, and shaking speed on adsorption behavior were systematically investigated. The data obtained were fitted into Langmuir, Freundlich, Dubinin-Rudishkevich (D-R), and Temkin adsorption isotherm models for evaluation of adsorption parameters. The results indicated that MRC-CNT nanocomposite would be a promising adsorbent for adsorption of Rh. B from aqueous solutions.

Keywords: nanocomposite, freundlich, dyes, characterization, adsorbent and adsorption

Introduction
The major challenge in water supply chain is continuous contamination of fresh water resources by a variety of pathogens, organic and inorganic pollutants. When these pollutants get into the environment they produce harmful effects to human beings and the environment [1]. Therefore, access to clean and safe drinking water is receiving huge attention and the necessity to improve and develop new and more efficient water cleaning processes has vastly intensified [2].
Organic contaminants in water include phenols, herbicides, pesticides, formaldehydes and dyes like Rhodamine B (Rh. B). Rh. B is a basic red cationic dye commonly used for commercial and industrial applications: Textile, printing and dyeing processes, paper manufacturing, rubber and plastic production and production of biological stains [3]. In addition to its application in dyeing industries, Rh. B in combination with Uramine-O (a basic dye) is used as a biological stain widely used in biomedical research laboratories as well as in the dyeing of leather and paper [4]. The indiscriminate discharge of Rh. B loaded effluents into water bodies introduces man, aquatic life and the environment to potentially harmful effects, ranging from minor irritations to major diseases [5]. Rh B is a very toxic dye and affects the growth and multiplication of aquatic life through depletion of dissolved oxygen [6]. Depletion of oxygen in water creates a viable environment for anaerobic bacteria to thrive [7]. These anaerobic bacteria produce toxic and smelly compounds like ammonia, amine, sulfide and flammable methane (mash gas) from nitrogen, sulphur and carbon which further contributes to environmental pollutions [8].

Further, Rh B contaminated water reduces the penetration of light to photosynthetic organisms affecting their growth and multiplication and also settles on the waterbed altering its characteristics making it unsuitable habitat for organisms [8]. This dye was considered for present work because it can cause skin dermatitis, allergic reaction, restlessness, hyperactivity, and attention problems. Exposure to this dye can cause irritation to nose, chemical conjunctivitis to eyes and hence its proper removal from water is mandatory. Therefore, the current study sought to synthesize functionalized mangrove roots charcoal-carbon nanotubes nanocomposite and explore its utilization as a novel adsorbent for the removal of Rh. B from aqueous solution.

Materials and Methods
Collection of Mangrove Roots and Functionalization of Carbon Nanotubes
Mangroves roots were used as an adsorbent and were collected from Dongo Kundu in Mombasa County. The samples were washed with water, dried, ground and the powder carbonized using 1.0 M $ZnCl_2$ at 500 ^oC for 3h. The purified CNTs was functionalized by using a mixture of 6 M sulfuric and 6 M nitric acid in a volume ratio of 1: 3 at 80 ^oC for 12 h and the nanocomposite was prepared by dispersing 1.2 g of functionalized MWCNTs in 100 ml deionized water containing MRC powder in the ratio of 1:3 by mass. The black product (MRC and CNTs mixture) obtained was washed with deionized water several times until a pH of 7.4 was obtained. The sample was dried overnight in a vacuum oven set at 80 ^oC. The fine powder was then stored in a desiccator for utilization.

Dye Solution Preparation
The dye Rh. B, molecular formula of $C_{28}H_{31}N_2O_3Cl$ and formula weight of 479.02 was used without further purification. An accurately weighed quantity of dye was

dissolved in double distilled water to prepare the stock solution (100 ppm). Serial dilutions were made by diluting it with double distilled water.

Batch Adsorption Experiments

The influences of initial adsorbate concentration (0–5 mg/L), contact time (0–60 min), pH (2–10), adsorbent dosage (2–50 mg), speed (0-600 rpm) and temperature (25–75 ºC) on the adsorption process were investigated. The batch mode adsorption experiments were conducted by bringing into contact the 50 mL of different Rh. B with a specified quantity of MRC-CNTs in a set of each 250 mL conical flasks. The concentration of residual Rh. B was then determined by Uv-vis spectroscopy (UV-Vis 1800 Shimadzu spectrophotometer). The Rh. B removal efficiency, R (%) and equilibrium amount of Rh. B adsorbed, qe, (mg/g), were calculated by Equations (1) and (2) below:

$$Q_e = \frac{(C_i - C_e)V}{m} \quad (1)$$

Where C_i and C_e are the initial and equilibrium concentrations (mg/L), *m* is the mass of the adsorbent (g) and *V* is the volume of the solution (mL).

$$\% \text{ Removal} = = \frac{C_0 - C_e}{C_0} \times 100 \quad (2)$$

Adsorption isotherm models

The correlation between the Amount of Rh. B adsorbed onto MRC-CNTs and the equilibrium concentration of Rh. B in the aqueous phase was evaluated using Langmuir, Freundlich isotherm, Dubin-Radushkevich and Temkin isotherms. The mathematical expression of Langmuir isotherm model is [9].

$$\frac{C_e}{q_e} = \frac{1}{Q_{max} b} + \frac{1}{Q_{max}} C_e \quad (3)$$

Where: q_e is the amount of solute adsorbed per unit weight of adsorbent (mg/g), C_e the equilibrium concentration of solute in the bulk solution (mgL^{-1}), Q_{max} the monolayer adsorption capacity (mgg^{-1}) and *b* is the Langmuir constant which reflects the binding strength between metal ions and adsorbent surface (Lmg^{-1}). The mathematical expression of Freundlich isotherm model is [10].

$$Log\ q_e = K_F + \frac{1}{n} \log C_e \quad (4)$$

Where: q_e is the amount of solute adsorbed per unit weight of adsorbent (mgg^{-1}), C_e the equilibrium concentration of solute in the bulk solution (mgL^{-1}), K_F a constant indicative of the relative adsorption capacity of the adsorbent (mgg^{-1}) and the constant 1/*n* indicates the intensity of the adsorption. The D-R equation is given by:

$$\ln q_e = \ln q_m - K_{DR} \varepsilon^2 \quad (5)$$

where Ɛ (Polanyi potential) is equal to RT ln(1+1/Ce); q_m is the maximum adsorption capacity (mg /g) based on D–R isotherm and K is related to mean adsorption energy (E in kilojoule per mole). The Temkin isotherm model is based on the assumption that the free energy of adsorption is a function of the surface coverage and the linear form is presented as follows [11].

$$q_e = B \ln A + B \ln C_e \quad (6)$$

where A (L/mg) is the equilibrium binding constant, the constant B= RT/b_T (mg/g) is related to the heat of adsorption, R is the ideal gas constant (8.314 J/mol K), T (K) is the absolute temperature and b_T is the Temkin isotherm constant.

Adsorption kinetic studies

The kinetic mechanism of the adsorption process was investigated by application of the pseudo-first order, pseudo-second order, intraparticle diffusion and liquid film diffusion model rate equations. Pseudo-first-order model is used to describe the reversibility of the equilibrium between solid and liquid phases [12] and is expressed by the equation shown below.

$$\log (q_e - q_t) = \log c_e - \frac{K_1}{2.303} t \quad (7)$$

Where: q_e and q_t are the amounts of heavy metal adsorbed ($mg\ g^{-1}$) at equilibrium and at the time (t min) and K_1 is the rate constant of the pseudo-first-order adsorption process (min^{-1}). Linear plots of log (q_e - q_t) versus t was used to predict the rate constant (K_1) and adsorption at equilibrium ($mg\ g^{-1}$), which are obtained from the slope and intercept respectively. The pseudo-second-order equation assumes that the rate limiting step might be due to chemical adsorption [13]. According to this model, adsorbates can bind to two binding sites on the adsorbent surface and the equation can be expressed as shown below.

$$\frac{t}{q_t} = \frac{1}{K_2 q_e^2} + \frac{1}{q_e} t \quad (8)$$

Where: K_2 is the rate constant of the pseudo-second-order adsorption ($gmg^{-1}min^{-1}$). If the adsorption kinetics obeys the pseudo-second-order model, a linear plot of t/q_t versus *t* can be observed. The intraparticle diffusion equation is given as follows [14].

$$q_t = K_d\ t^{\frac{1}{2}} + C \quad (9)$$

Where K_d ($mg\ g^{-1}\ min^{-1/2}$) is the intraparticle diffusion rate constant and *C* represents the intercept and is related to the thickness of the boundary layer. When the transport of the adsorbate from the liquid phase to the solid phase boundary plays the most significant role in adsorption, then the liquid film diffusion model can be applied [15].

$$\ln(1-F) = -K_{fd} + Y \quad (10)$$

Where $F = \frac{q_t}{q_e}$ is the fractional attainment of equilibrium, K_{fd} (mg/g min) is the film diffusion adsorption rate constant and Y is the intercept. A linear plot of ln (1– F) versus t suggests that the kinetics of adsorption involves a film diffusion mechanism. Furthermore, if the plot is linear with (Y = 0) then film diffusion is the sole rate controlling mechanism.

Results and Discussions

Effect of MRC -CNTs weight on adsorption of Rh. B dye

In the current study, it was observed that the percentage removal of Rh. B dye increased as the MRC-MWCNT dosage increased over the range of 10 to 60 mg as shown in Figure 1

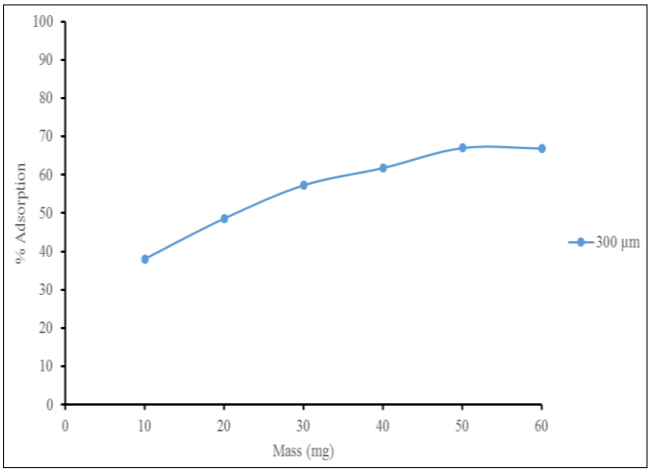

Fig 1: Effect of MRC-CNTs Nanocomposite weight on % adsorption of 5 ppm Rh. B Dye.

The rapid uptake of metal ions on the adsorbent may indicate that most of the reaction sites of the adsorbent were exposed for interaction with Rh. B molecules [16]. Furthermore, the presence of hydroxyl group on adsorbent surface forms a complex between Rh. B molecule and adsorbent surface causing faster adsorption [17].

Effect of initial concentration of Adsorbates on adsorption

The effect of initial Rh. B concentrations (2, 4, 6, 8, and 10.0 mgL^{-1}) on the adsorption of Rh. B onto the MRC-CNTs was studied using mass of 50 mg and the dye solution at room temperature and natural pH.

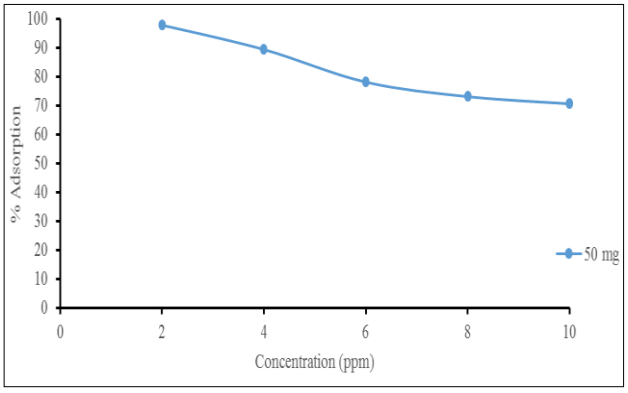

Fig 2: Effect of Initial Rh. B Concentration on Adsorption by 50 mg MRC-CNTs Nanocomposite

According to Figure 2 above, the percentage removal of MRC-CNTs decreased from 97.95% to 70.7% when the initial dye concentration increased from 2 to 10 $mg{\cdot}L^{-1}$. These results shows that adsorption is highly dependent on initial concentration of adsorbates. This observation can be explained by the fact that at lower concentration, the ratio of the initial number of Rh. B molecules to the available adsorbent surface area is low and subsequently the functional adsorption became independent of initial concentration. However, at higher concentration, the available sites of adsorption become fewer and hence the percentage removal of Rh. B is dependent upon initial concentration [18].

Effect of Contact Time on Adsorption of Rh. B Dye

Contact time is an important factor that affect the removal of adsorbates from aqueous solutions. Figure 3 shows plots of % adsorption of Rh. B Dye onto MRC-CNTs nanocomposite versus contact time.

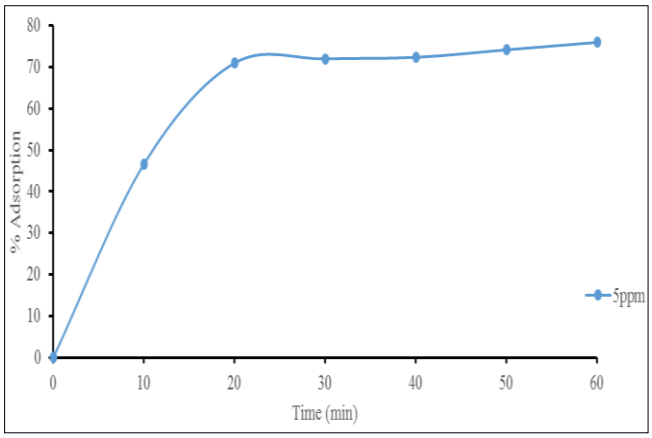

Fig 3: Effect of Contact Time on Adsorption of Rh. B onto 50 mg of MRC-CNTs Nanocomposite

As seen in Fig. 3, % adsorption increases evidently from 46.6 to 75.98 % for a contact time of 10 minutes to 60 minutes. The adsorption rate increased with time at the initial stage and became slower before reaching equilibrium. This can be attributed to the fact that vacant sites were available on the adsorbents at the initial stage. This developed a strong driving force for dye molecules to overcome the mass transfer resistance between aqueous and solid phases.

After a period of time, the remaining surface site became difficult to occupy due to the electrostatic hindrance or repulsive forces that exist between the dye molecules and the surface of adsorbent. At this point, equilibrium was reached and this stage also reflects the maximum adsorption capacity of the adsorbent under certain operating conditions.

Effect of Shaking Speed on Adsorption of Rh. B Dye

The effect of variation in stirring speed on adsorption of Rh. B onto MRC-CNTs was studied over the range of 0 to 800 rpm while keeping other parameters such as the adsorbent dosage at 50 mg, the initial concentration of 5 mg/L, room temperature and the natural pH of the solutions constant.

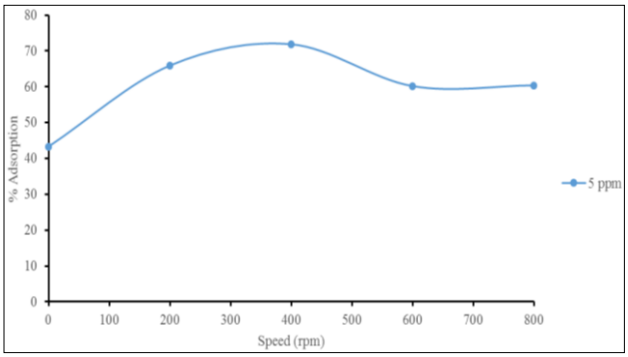

Fig 4: Effect of Shaking Speed on adsorption of 5 ppm Rh. B on 50 mg of MRC-CNTs Nanocomposite

The highest adsorption of 71.88% was obtained at 400 rpm whereas the lowest was 60.2 at 600 rpm as shown in Figure 4. It was observed that adsorption yield increased with increase in stirring speed up to the optimal level and further rise in stirring speed resulted to decline the adsorption efficiency. This could be explained by the fact that agitation results in an increase in ion mobility in the solution and reduces the mass transfer resistance leading to high percentage removal of dye molecules [19]. At high agitation speed, boundary layer becomes thinner, which usually improves the rate of solute diffusion through the boundary layer and as a result the percentage removal increases. However, for very high agitation speeds (> 400 rpm) the adsorbent and adsorbates do not have enough contact time for reaction to take place and as a result the percentage removal of Rh. B dye declines.

Effect of pH on Adsorption of Rh. B ions

To investigate the effect of solution pH on dye removal efficiency, the pH of the solution was varied from 2 to 10, while the dye concentration was kept constant at 5 mg/L. The obtained results are presented in Figure 5.

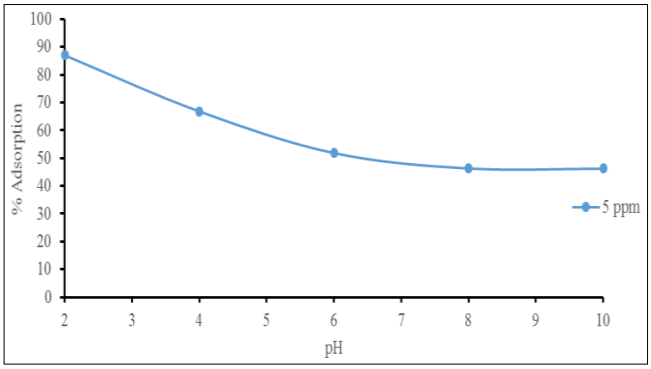

Fig 5: Effect of pH on the % Adsorption of 5 ppm Rh. B by 50 mg of MRC-CNTs Nanocomposite

The results showed that, as the pH increased from 2 to 10, the dye removal efficiency drastically decreased from 86.98 to 46.2 % after a contact time of 30 min. The amount of dye adsorbed on the surface of the adsorbent is influenced by the adsorbent surface charge and consequently solution pH. Rh. B exists in two forms; cationic and zwitterionic in polar solvents and the transformation of the cationic to zwitterionic form occurs by deprotonation of the carboxyl group of the cationic Rh. B form [20]. Electrostatic interactions between the functional groups on the adsorbent and the carboxyl group of Rh. B monomers causes the aggregation of Rh. B to form dimers and hinders the adsorption of dye molecules into the pores. As a result, the % removal of dye adsorbed on the MRC-CNTs nanocomposite decreased with an increase in pH of the solution.

Adsorption Isotherm Studies for Rh. B Dye

Four adsorption isotherms were used in the current study to study the adsorption process. These are Langmuir, Freundlich, D-R and Temkin adsorption isotherm. The Langmuir, Freundlich, Temkin and D-R isotherm parameters were determined through the linearized form and their values, along with the respective correlation coefficients listed in Table 1. By comparing the correlation coefficient (R^2) obtained from four adsorption models, it can be observed that the Freundlich model provides the best fitness for the adsorption of the Rh. B molecules onto MRC-CNTs. The appropriateness of the Freundlich model to the experimental data signifies multilayer capacities on the MRC-CNTs surface by Rh. B. Similar results were obtained by [21].

Table 1: Langmuir, Freundlich, Dubinin–Radushkevich and Temkin model parameters for Rh. B dye adsorbed onto 50 mg MRC-CNTs nanocomposite. (Weight of adsorbent=50 mg, agitation speed=300 rpm, contact time=30 min, pH=natural, room temperature).

Langmuir				**Freundlich**		
Q_{max}(mg g^{-1})	*b*(L mg^{-1})	R^2	R_L	K_F(mg g^{-1})	n	R^2
6.784	0.4565	0.9816	0.3046	3.2898	3.1826	0.9854
Dubin- Radushkevich				Temkin		
Q_m (mg g-1)	E ($Kjmol^{-1}$)	R^2		A (L mg^{-1})	b_T	R^2
0.1383	3.752	0.9457		19.2248	3048.19	0.8202

Adsorption Kinetics of Rh. B Dye

Adsorption kinetics was studied to understand the dynamics of the system, applying pseudo-first and pseudo-second-order, intraparticle diffusion and liquid film diffusion model. From Table 2, coefficient correlation value (R^2= 0.8056) of pseudo-first order model was low as compared to that of pseudo-second order (0.9909). This suggests that the adsorption of Rh. B molecules does not follow pseudo-first-order kinetics properly.

Pseudo-second-order model is based on the assumption that the rate-limiting step may be chemical adsorption that involves valence forces through sharing or an exchange of electrons between adsorbates molecules and the adsorbents, hence offers the best consistent data for the Rh. B [22]. It was also found that the model predicted q_e values (1.5733 mg/g) agree well with experimental q_e values (1.44 mg/g) for adsorption of Rh. B molecules onto MRC-CNTs as shown in Table 2. This suggests that the pseudo second-order kinetic model portray that the Rh. B molecules adsorption onto MRC-CNTs is a rate-limiting step and the chemical adsorption may involve by valance forces through sharing or exchange of electrons between Rh. B and the adsorbent**.**

Adsorption kinetics data from Rh. B molecules adsorption onto MRC-CNTs were further used to define whether the intra-particle diffusion is rate limiting and also to find the diffusion constant rate, k_p (mg/g $min^{0.5}$). Intraparticle diffusion model is presented by the relationship between specific adsorption and the square root of time, according to equation 9. It is evident from Figure 13 that the plot is

multi-staged. The first stage may be attributed to the boundary layer diffusion effect, while the second stage may be due to intra-particle diffusion effects [23]. Therefore, the slope of the top portion which has a linear portion may be defined as a rate parameter (k_p) and a characteristic of the adsorption rate in the region, where intra-particle diffusion was reported to be the rate-limiting factor for Rh. B adsorption onto MRC-CNTs.

Table 2: Pseudo-First-Order, Pseudo–Second-Order, Intra particle diffusion and Liquid film diffusion Rate Constants for Adsorption of Rh. B ions on 50 mg MRC-CNTs Nanocomposite

Pseudo-first-order				**Pseudo-second -order**		
[Rh. B] mg/L	$Q_{e(mg/g)}$	Constant (min^{-1})	R^2	Q_e(mg/g)	Constant (g/mg/min)	R^2
5	0.0654	0.05896	0.8056	1.5733	0.21773	0.9909
Intraparticle diffusion				Liquid film Diffusion		
Rh. B (ppm	C(mg g^{-1})	K_d(mg g^{-1} $min^{-1/2}$)	R^2	Intercept	K_{fd}(mg/gmin)	R^2
5	0.7646	0.1067	0.6868	2.2402	0.019	0.9503

Conclusions

In the current study, the ability of MRC-CNTs nanocomposite to remove Rh. B from aqueous solution was investigated. It was found that the prepared MRC-CNTs acted as an effective adsorbent for the removal of Rh. B with adsorption capacity of 1.5733mg/g which was calculated by the Pseudo Second Order.

Recommendations

The following recommendations were made for future study:

1. A pilot-scale column with the developed adsorbent can be conducted for real water.
2. A suitable modification method for preparing adsorbents can be considered to obtain maximum removal of dyes.
3. The performance of removal of dyes along with other organic pollutants like pesticides and nitrates can be evaluated by using the developed adsorbents.

Acknowledgment

My gratitude goes to Tharaka University College for provision of Research Fund to facilitate this research work.

References

1. Jaya kumar NS, Mubarak NM, Sahu JN, Abdullah, CE. Removal of Heavy Metals from Wastewater Using Carbon Nanotubes, Separation & Purification: Review, Journal of Environmental Science. 2013; 43(4):311-338,
2. Nyairo WN, Eker YR, Kowenje C, Akin I, Bingol H, Tor A et al. Efficient adsorption of lead (II) and copper (II) from aqueous phase using oxidized multiwalled carbonnanotubes/polypyrrole composite, Separation Science and Technology, 2018, 1520-1527.
3. Kumar S, Bhanjana SG, Jangra K, Dilbaghi N, Uma A. Utilization of Carbon Nanotubes for the Removal of Rhodamine B Dye from Aqueous Solutions. Journal of Nanoscience and Nanotechnology. 2013; 13:1-7.
4. Bello SO, Lasisi BM, Adigun JO, Ephrahim V. Scavenging Rhodamine B dye using moringa oleifera seed pod. Chemical Speciation & Bioavailability. 2017; 29(1):120-134.
5. Oyetade AO, Nyamori OV, Martincigh SB, Jonnalagadda BS. Effectiveness of Carbon Nanotubes-Cobalt Ferrite Nanocomposites for the Adsorption of Rhodamine B from Aqueous solutions. Royal Society of Chemistry. 2015; 5:22724-22739.
6. Salman M, Athar M, Shafique U, Rehman R, Ameer S, Ali SZ et al. Removal of Formaldehyde from Aqueous Solution by Adsorption on Kaolin and Bentonite: A Comparative Study. Journal of Engineering and Environmental Science. 2012; 36:263-270.
7. Huihui L, Cai X, Wanga Y, Jingwen C. Adsorption Mechanism-based screening of Cyclodextrin Polymers for Adsorption and Separation of Pesticides from Water. *Water Research*. 2011; 45:3499-3511.
8. Rashed MN. Adsorption Technique for the Removal of Organic Pollutants from Water and Wastewater. Journal of Hazardous Material. 2010; 8(6):48-72.
9. Aravind J, Shanmuga prakash M, Sangeetha HS, Lenin C, Kanmani P. Pigeon Pea (Cajanuscajan) Pod as a Novel Eco-Friendly Biosorbent: A Study on Equilibrium and Kinetics of Ni (II) Biosorption. International Journal of Industrial Chemistry. 2013; 4:1-25.
10. Ahmad AA, Hameed BH. Reduction of COD and Color of Dyeing Effluent from Cotton Textile Mill by Adsorption onto Bamboo-based Activated Carbon. Journal of Hazardous Materials. 2009; 172:1538-1543.
11. Akpomie KG, Dawodu AF. Treatment of an Automobile Effluent from Heavy Metals Contamination by an Ecofriendly Montmorillonite. Journal of Advanced Research. 2015; 6:1000-1013.
12. Vijaya K, Yun VS. Bacterial Biosorbents and Biosorption. Biotechnology Advances. 2008; 26:266-291.
13. Amboga DA, Onyari JM, Shiundu PM, Gichuki JW. Equilibrium and Kinetics Studies for the Biosorption of Aqueous Cd (II) ions onto Eichhornia crassipes Biomass. *Journal of Applied Chemistry*. 2014; 7(1):29-37.and equilibrium isotherm analyses. *Dyes Pigments* 69(3):210–223
14. Kooh RRM, Dahri KM, Lim BLL. The Removal of Rhodamine B dye from Aqueous Solutions using Casuarinaequisetifolia Needles as Adsorbent. Cogent Environmental Science. 2016; 2:1-14.
15. Taffarel SR, Rubio J. On the Removal of Mn Ions by Adsorption onto Natural and Activated Chilean Zeolites. Journal of Mineral and Engineering. 2009; 22:336-343.
16. Li X, Yunjin L. Adsorptive Removal of Dyes from Aqueous Solution by KMnO4-Modified Rice Husk and Rice Straw. Journal of Chemistry, 2019, 9.
17. Tang R, Dai C, Li C, Liu w, Gao S, Wang C et al. Removal of Methylene Blue from Aqueous Solution Using Agricultural Residue Walnut Shell: Equilibrium, Kinetic, and Thermodynamic Studies, Hindawi Journal of Chemistry, 2017, 10.
18. Kuang Y, Zhang X, Zhou S. Adsorption of Methylene

Blue in Water onto Activated Carbon by Surfactant Modification, Water. 2020; 12:587-606.
19. Ngugi F, Onyari JM, Wabomba NM. School of Physical Sciences, College of Biological and Physical Sciences, University of Nairobi, P.O. Box 30197- 0100, Nairobi, Kenya. Efficacy of Mangrove (Rhizophora Mucronata) Roots Powder in Adsorption of Lead (II) Ions from Aqueous Solutions: Equilibrium and Kinetics Studies IOSR Journal of Applied Chemistry (IOSR-JAC). 2016; 9(8):45-51.
20. Mohammadi M, Hassani JA, Mohamed AR, Najafpour GD. Removal of Rhodamine B from Aqueous Solution Using Palm Shell-Based Activated Carbon: Adsorption and Kinetic Studies Journal of Chemical Engineering. 2010; 55:5777–5785
21. Al-Senani GM, Al-Fawzan FF. Adsorption study of heavy metal ions from aqueous solution by nanoparticle of wild herbs. Egyptian Journal of Aquatic Research. 2019; 44:187-194
22. Inam E, Etimb UJ, Akpabio EG, Umoren SA. Process optimization for the application of carbon from plantain peels in dye abstraction, Journal of Taibah University for Science. 2016; 12(4):567-577.
23. Solic M, Maletic S, Isakovski MK, Niki J, Watson M, Kónya Z et al. Comparing the Adsorption Performance of Multi walled Carbon Nanotubes Oxidized by Varying Degrees for Removal of Low Levels of Copper, Nickel and Chromium(VI) from Aqueous Solution, Water. 2020; 12:723.